Vol. 13, pp. 321–331 (2016)
doi: 10.2142/biophysico.13.0_321

Biophysics and Physicobiology
https://www.jstage.jst.go.jp/browse/biophysico/

Regular Article

Actin binding domain of filamin distinguishes posterior from anterior actin filaments in migrating *Dictyostelium* cells

Keitaro Shibata[1,4], Akira Nagasaki[1], Hiroyuki Adachi[2] and Taro Q. P. Uyeda[1,3]

[1]*Biomedical Research Institute, National Institute of Advanced Industrial Science and Technology, Tsukuba, Ibaraki 305-8562, Japan*
[2]*Department of Biotechnology, University of Tokyo, Bunkyo-Ku, Tokyo 113-8657, Japan*
[3]*Department of Physics, Faculty of Science and Engineering, Waseda University, Shinjuku, Tokyo 169-8555, Japan*
[4]*Present address: Department of Biology, University of Padova, Padova 35121, Italy*

Received August 25, 2016; accepted November 28, 2016

Actin filaments in different parts of a cell interact with specific actin binding proteins (ABPs) and perform different functions in a spatially regulated manner. However, the mechanisms of those spatially-defined interactions have not been fully elucidated. If the structures of actin filaments differ in different parts of a cell, as suggested by previous *in vitro* structural studies, ABPs may distinguish these structural differences and interact with specific actin filaments in the cell. To test this hypothesis, we followed the translocation of the actin binding domain of filamin (ABD_{FLN}) fused with photoswitchable fluorescent protein (mKikGR) in polarized *Dictyostelium* cells. When ABD_{FLN}-mKikGR was photoswitched in the middle of a polarized cell, photoswitched ABD_{FLN}-mKikGR rapidly translocated to the rear of the cell, even though actin filaments were abundant in the front. The speed of translocation (>3 μm/s) was much faster than that of the retrograde flow of cortical actin filaments. Rapid translocation of ABD_{FLN}-mKikGR to the rear occurred normally in cells lacking GAPA, the only protein, other than actin, known to bind ABD_{FLN}. We suggest that ABD_{FLN} recognizes a certain feature of actin filaments in the rear of the cell and selectively binds to them, contributing to the posterior localization of filamin.

Key words: photoswitchable fluorescent protein (mKikGR), structural polymorphism

Corresponding author: Taro Q. P. Uyeda, Department of Physics, Faculty of Science and Engineering, Waseda University, 3-4-1 Okubo, Shinjuku, Tokyo 169-8555, Japan.
e-mail: t-uyeda@waseda.jp

Actin is a ubiquitous cytoskeletal protein that plays important roles in various cellular activities such as cell migration, cell division and intracellular transport in eukaryotic cells [1–4]. Each of the multiple functions of actin is dependent on interactions with specific actin binding proteins (ABPs). Interaction with the Arp2/3 complex, for example, produces a dendric meshwork of actin filaments in sheet-like pseudopods called lamellipods at the front of migrating cells, and polymerization of actin filaments in this dendric meshwork extends the lamellipods forward. The length of lamellipods is controlled by cofilin, which severs and depolymerizes actin filaments at the back of lamellipods. Additionally, actin filaments form a cortical network underlying the cell membrane, and interact with focal adhesions through linker proteins. Myosin II filaments produce a contractile force at the rear of the cell by pulling the network of actin filaments [5,6]. An advance of the leading lamellipods and contraction

◀ ***Significance*** ▶

It is not well understood how different actin filaments interact with different actin binding proteins (ABPs) in a spatially regulated manner. Here, we demonstrate that the actin binding domain of filamin (ABD_{FLN}) in the middle of elongated, polarized *Dictyostelium* cells rapidly and specifically binds to posterior actin filaments. The speed of translocation was much faster than the retrograde flow of actin cortex, suggesting that ABD_{FLN} diffusing in the cytoplasm was captured by posterior actin filaments. We suggest that this specific interaction depends on structural polymorphism of actin filaments, and a similar mechanism may contribute to intracellular localization of other ABPs.

of the rear cooperatively drives movement of an amoeboid cell. Thus, actin filaments interact with various ABPs and perform different functions in a spatially regulated manner in a cell. It is generally believed that the spatially-defined interactions between actin filaments and ABPs are controlled by local biochemical regulation of each ABP, but there are a number of cases in which such simple biochemical explanations are unknown or insufficient.

Notably, the cortical actin network continuously moves toward the rear of a polarized cell during cell migration, in part driven by contraction of actin and myosin in the rear [7–10]. Recent measurements in the cellular slime mold *Dictyostelium discoideum* demonstrated that the speed of this rearward cortical flow, or retrograde flow, is similar to that of the forward movement of polarized cells [6], such that the cortical actin meshwork is stationary relative to the substrate during movement. Nonetheless, there is a rapid turnover of cortical actin filaments within seconds, and it is not that the same group of actin filaments remain stationary to the substrate [6].

Dictyostelium filamin, an orthologue of human filamin, is a dimeric ABP with actin cross-linking activity. The meshwork of actin filaments cross-linked by filamin is important for cell migration, chemotaxis and mechanosensing [11–14]. Each filamin polypeptide has an actin binding domain (ABD) consisting of two calponin homology (CH) domains at the N-terminus, a rod domain, and a dimerization domain at the C-terminus [15,16]. ABD_{FLN} interacts with actin filaments with high affinity allowing ABD_{FLN} to be fused with green fluorescent protein (GFP) to visualize actin filaments *in vivo* [6,17,18]. In polarized cells, filamin is localized in the posterior region [14,19,20]. Moreover, filamin tends to localize at stretched actin filaments *in vivo* [13]. It is possible that this property contributes to the control of force transmission and rigidity sensing by filamin [11,12,21]. However, it is not known how filamin distinguishes and interacts with specific actin filaments in a cell.

Each actin protomer in a filament assumes one of the multiple structures depending on its nucleotide state, applied mechanical stress and/or interactions with ABP [22–32]. Binding of cofilin induces a cooperative structural change of actin protomers in filaments that involves supertwisting of the helix. This cooperative structural change enhances the affinity of affected actin protomers for cofilin, resulting in cooperative binding of cofilin [26,28,30]. Conversely, stretching actin filaments inhibits their interaction with cofilin but enhances their interaction with myosin II [5,28,33,34]. Additionally, there is some evidence that certain ABPs, including cortexilin [35,36], fimbrin [24,37], and drebrin [29,38], selectively interact with actin filaments of a specific structure. Along this line, we recently showed that binding of the motor domain of myosin II in the presence of ATP induces a conformational change in actin filaments to reduce the affinity for cofilin, while the supertwisted actin filaments induced by cofilin binding has a lower affinity for the myosin motor domain [39]. Thus, the structure of actin protomers in filaments is potentially an important factor for selective binding of ABPs.

Here, we hypothesized that ABD_{FLN} accumulates in the rear of polarized cells by recognizing a certain structural feature of specific actin filaments in the rear of cells. To test this hypothesis, we followed the translocation of ABD_{FLN} using a photoswitchable fluorescent protein, monomeric kikume green-red (mKikGR), in polarized *Dictyostelium* cells [40]. Use of ABD, pioneered by Washington and Knecht [19], eliminates the possible contribution of dimeric filamin molecules by recognizing the orthogonal arrangement of actin filaments [2,15,16,21], and may reduce the contribution of biochemical regulation in actin binding because *Dictyostelium* ABD_{FLN} is not known to be influenced by phosphorylation or by other biochemical regulations. Photoswitching of mKikGR from green to red fluorescence by local irradiation with purple light allows observation of translocation of ABD_{FLN} from the irradiated area to other places. We found that the majority of red ABD_{FLN}-mKikGR molecules generated in the middle of an elongated cell translocated to the cell rear at a much faster speed than the retrograde flow of cortical actin filaments, even though actin filaments were equally or more abundant in the front of cells. The result suggests that ABD_{FLN} recognizes a certain feature of actin filaments in the cell rear, and selectively binds to those filaments.

Materials and Methods

Construction of plasmids

pTX/ABD-fluorescent protein: Coding sequences of ABDs of filamin and α-actinin of *Dictyostelium discoideum* were subcloned into a modified pTX-GFP vector [41], from which sequences coding 8xHis, GFP and myc had been removed. Then, the coding sequence of GFP (from pTX-GFP) or mKikGR (from CoralHue® phmKikGR1-MCLinker, Molecular and Biological Laboratories) preceded by a linker (GSGGGGS) was inserted downstream of the ABD sequence of pTX/ABD.

pDdBsr/mCherry-lifeact: Lifeact [42] fused to the C-terminus of mCherry, was subcloned in pDdBsr [5], and expressed under the control of the actin15 promoter.

pBIG GFP-GAPA: The coding sequence of *Dictyostelium gapA* was inserted downstream of GFP in pBIG GFP [43].

Cell culture and expression of ABD-fluorescent protein

Wild-type *D. discoideum* AX2 cells and GAPA null cells [44] were cultured in HL5 medium supplemented with penicillin and streptomycin [45], and transfected by electroporation with the pTX/ABD-fluorescent protein, pDdBsr/mCherry-Lifeact and/or pBIG GFP-GAPA as described previously [46]. Transfectants were selected by 20 μg/mL G418 and/or 6 μg/mL blasticidin S in HL-5 medium at 22°C.

Live cell imaging and photoswiching of mKikGR under a confocal microscope

Cells expressing ABD-fluorescent proteins and/or mCherry-Lifeact were settled on glass-bottomed dishes (Matsunami, 35 mm dish, hole size: 27 mm, uncoated). To obtain polarized cells, the cells were then starved in 10 mM K^+-Na^+-phosphate buffer (pH 6.4) until chemotaxis started (~11–12 h at 22°C or ~14–16 h at 11°C). To obtain images of flattened cells, the polarized cells were overlaid with a thin agarose sheet, as described previously [47]. The flattened and polarized cells were observed with a confocal microscope (Zeiss, LSM700) equipped with a 100x objective lens (Zeiss, Plan-Neofluar 100x/1.30 Oil Iris). LED lasers (488 nm: 10 mW, 555 nm: 10 mW) were used for scanning the cells, and images were acquired with ZEN imaging software (Zeiss). The duration for a single frame acquisition was 4~5 s, depending on the size of scanned area. The pinhole size was 1 AU (airy unit) (1 AU = 74.20 µm for the 488 nm laser, 79.74 µm for the 555 nm laser). To prevent photobleaching and affecting cell motility, the excitation laser power was set at minimum value (0.5%).

Cells expressing both ABD-GFP and mCherry-Lifeact were irradiated with the 488 nm and 555 nm laser light simultaneously, and those expressing ABD-mKikGR were sequentially irradiated with the 488 nm and 555 nm laser light. The resultant green fluorescence from GFP or mKikGR and red fluorescence from mCherry or mKikGR were separated by a variable secondary dichroic beam splitter (Carl Zeiss) and emission filters, and also a differential interference contrast (DIC) image was simultaneously acquired with each frame. For photoswitching of mKikGR, square areas were scanned four times repeatedly by 405 nm LED laser light (5 mW, 100% laser power). Fluorescence intensities along the cell cortex were analyzed with ZEN and ZEN lite imaging software (Zeiss), as follows. For each cell image, a 1 µm wide band was drawn manually along the cell periphery in the DIC image, such that the cell periphery ran along the center of the band. This band is shown as a thick white line in each cell image. Then the intensities of red and green fluorescence were measured along the length of the band. Each cell type in this report was analyzed in 4–5 independent experiments, and more than 3 cells were observed in each experiment. Rapidly migrating and well-separated polarized cells were selected for observation.

Correction of red fluorescence intensity of ABD-mKikGR

There was weak but non-negligible fluorescence in the red channel from ABD_{FLN}-mKikGR-expressing cells not irradiated with 405 nm laser light. It was thus necessary to subtract this red fluorescence from the image of irradiated cells, in order to extract red fluorescence intensity that was derived from photoswitching by irradiation. For this purpose, a correction coefficient was obtained for each cell from a plotted graph of the green and red fluorescence intensities at the same points along the cell cortex before irradiation with 405 nm light (Supplementary Fig. S1). This coefficient and the fluorescence intensity in the green channel at each pixel were used to estimate fluorescence intensity in the red channel that derived from ABD-mKikGR that was not photoswitched by irradiation. This value was subtracted from the fluorescence intensity in the red channel at that pixel.

Observation of fixed cells

Polarized cells prepared as above were permeabilized and fixed by changing the K^+-Na^+-phosphate buffer (pH 6.4) to PF buffer (10 mM Pipes-KOH pH 6.8, 3 mM $MgCl_2$, 1 mM EGTA, 1 mM DTT, 0.05% Triton X-100, 0.1% glutaraldehyde, 1% formaldehyde) and incubated for 5 min at 22°C, followed by incubation in 10 mM Tris-HCl pH 7.0, 3 mM $MgCl_2$, 1 mM EGTA, and 1 mM DTT for 5 min. Then, they were stained for 1 h in PBS containing 3 nM rhodamine-phalloidin (Invitrogen), rinsed in PBS containing 10 mM DTT, and observed with an LSM 700 microscope.

Results

Localization of ABD-GFP

Localization of ABD_{FLN} fused with GFP at the C terminus (ABD_{FLN}-GFP) via a Gly-based linker (GSGGGGS) was observed in polarized *Dictyostelium* cells with a confocal fluorescence microscope (Fig. 1A and Supplementary Fig. S2). Actin filaments were visualized by expression of lifeact [42] fused with mCherry at the N terminus (mCherry-lifeact). To compare the localization of ABD_{FLN} with that of actin filaments more quantitatively, the fluorescence intensities of the images of Figure 1A were measured along the cell cortex (Fig. 1B). Although ABD_{FLN}-GFP colocalized with actin filaments, it localized more intensely in the rear of the cell (Fig. 1B: at ~0 µm) than in the front (Fig. 1B: at ~–20 and ~20 µm). This is indicated by the magenta color of the cell front in the merged image (Fig. 1A), as well as by the ratio of GFP fluorescence intensity to that of mCherry (Fig. 1E: purple line, and Supplementary Fig. S3A), and is consistent with the previous study by Washington and Knecht [19].

Next, the localization of α-actinin ABD (ABD_{ACTN}) was observed (Fig. 1, C and D and Supplementary Fig. S2) to compare with the localization of ABD_{FLN}-GFP, because ABD_{ACTN} consists of two CH domains and is homologous to ABD_{FLN}. A previous report showed that accumulation of GFP-ABD_{ACTN} in actin-rich structures is weaker than that of GFP-ABD_{FLN}, and discernable localization in actin-rich structures was observed only when the ABD_{ACTN} is in oligomers such as dimers and tetramers [20]. In this study, monomeric ABD_{ACTN}-GFP showed almost the same distribution as actin filaments along the cortex (Fig. 1, C and D and orange line in E), although the localization signal along the cortex was not very strong relative to that of cytosol (Supplementary Fig. S3, D and H). GFP alone was only diffusely distributed in the cytoplasm (Fig. 1F). These results suggest that ABD_{FLN} shows strong preference for rear actin filaments, but

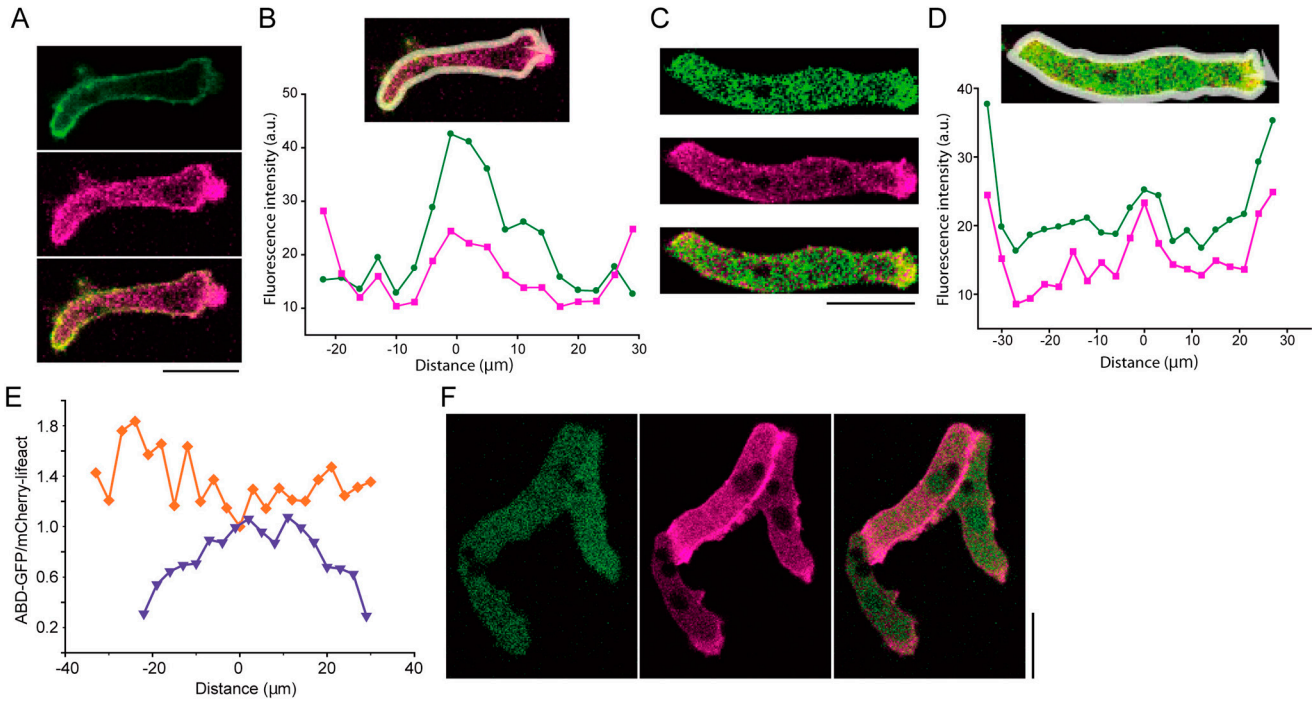

Figure 1 Localization of actin filaments and ABDs fused with GFP. (A) Fluorescence micrographs of a polarized cell expressing ABD_{FLN}-GFP (top), mCherry-lifeact (middle) and the merged image (bottom). (B) Intensity profile of each fluorescence along the cortex, measured along the white line in the direction of the arrow in the merged image (inset, the same cell as in A) with the 0 μm set at the rear end. Green and magenta lines show the intensity of ABD_{FLN}-GFP and mCherry-lifeact, respectively. (C) Fluorescence micrographs of a polarized cell expressing ABD_{ACTN}-GFP (top), mCherry-lifeact (middle) and the merged image (bottom). (D) Intensity profile of each fluorescence along the cell cortex, measured along the white line in the direction of the arrow in the merged image (inset, the same cell as in C) with the 0 μm set at the rear end. Green and magenta lines show the intensity of ABD_{ACTN}-GFP and mCherry-lifeact, respectively. (E) Ratio of the fluorescence intensity of ABD-GFP to that of mCherry-lifeact along the white lines in the merged images. The purple line shows ABD_{FLN}-GFP : mCherry-lifeact, and the orange line shows ABD_{ACTN}-GFP: mCherry-lifeact. The intensity ratios at the rear end of the cells are set at 1. (F) Fluorescence micrographs of polarized cells expressing GFP (left), mCherry-lifeact (middle) and the merged image (right). Cells of (A) and (C) migrated toward the right of the images and cells of (F) migrated downward. Scale bars: 10 μm. Additional representative cells of each condition are shown in Supplementary Figure S2.

this is not a general property of ABDs consisting of two CH domains.

Localization of ABD_{FLN}-mKikGR

To investigate the mechanism by which ABD_{FLN} localizes at the rear of a cell, we next followed the translocation of ABD_{FLN} real time by observing ABD_{FLN}-mKikGR in polarized cells with a confocal microscope (Fig. 2, A and B and Supplementary Fig. S4). A pair of green and red fluorescence images was obtained by scanning with 488 nm laser light followed by 555 nm laser light. The green fluorescent ABD_{FLN}-mKikGR, which is the native state of this fluorescent protein in the absence of photoswitching by irradiation with 405 nm light, showed stronger accumulation in the rear of a cell than ABD_{FLN}-GFP (Fig. 2A; at –4.9 s). Additionally, weak red fluorescence was also detected in the rear even without photoswitching (Fig. 2B; at –4.9 s). This is presumably due to very strong accumulation of ABD_{FLN}-mKikGR in the cell rear. Red fluorescence might derive from native mKikGR that is weakly excited by 555 nm light and bled through the red emission filter. Alternatively, a small, background fraction of mKikGR was in the red fluorescent state due to ambient light or by spontaneous conversion.

To locally photoswitch ABD_{FLN}-mKikGR in a polarized cell, the area bound by the yellow square in Figure 2A and B was scanned by 405 nm laser light for ~0.4 s. The red fluorescent ABD_{FLN}-mKikGR generated near the center of the polarized cell spread in the area slightly posterior to the irradiated area and more intensely at the rear of the cell (Fig. 2, A and B). Fluorescence intensity along the cell cortex was measured to reveal the movement of ABD_{FLN} during this process (Fig. 2, C and D). In addition, the intensity profile of the observed red fluorescence of ABD_{FLN}-mKikGR was corrected by subtracting the red fluorescence that was unrelated to irradiation with 405 nm light (see Materials and Methods). Since neighboring cells in the same microscopic field not irradiated with the 405 nm laser light did not show an increase in red fluorescence, the 488 or 555 nm laser light did not contribute to the generation of red fluorescent ABD_{FLN}-mKikGR (Supplementary Fig. S5). Therefore, this procedure extracted the red fluorescence of ABD_{FLN}-mKikGR generated by 405 nm laser light irradiation in the boxed area (Fig. 2D).

Accumulation of red fluorescent ABD_{FLN}-mKikGR in the

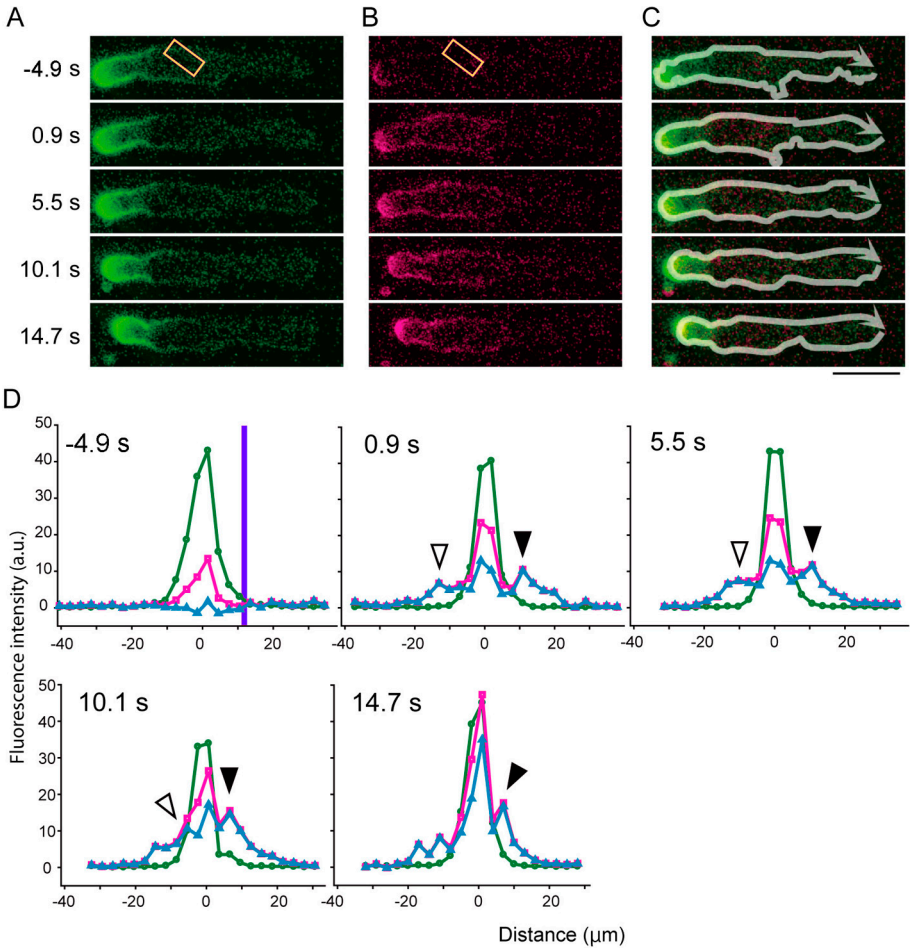

Figure 2 Translocation of ABD_{FLN}-mKikGR. Time lapse images of a polarized cell expressing ABD_{FLN}-mKikGR and migrating toward the right (A, B and C). (A) and (B) show the green and red fluorescence images of mKikGR, respectively, and (C) shows the merged images. The region bound by the yellow square was irradiated by 405 nm laser light for 0.38 s immediately after taking the pre-irradiation image (–4.9 s). Scanning for subsequent images were started at 0.9, 5.5, 10.1, and 14.7 s after starting the 405 nm laser irradiation, which was set as time = 0. Scale bar: 10 μm. (D) Profiles of fluorescence intensity along the cell cortex shown by the white arrows in (C), with the 0 μm set at the rear end. The green and magenta lines show fluorescence intensities of ABD_{FLN}-mKikGR in the green and red channels, respectively. The cyan lines show red fluorescence intensities of ABD_{FLN}-mKikGR after subtracting the fluorescence intensities in the red channel that were unrelated to stimulated photoswitching. The purple vertical bar in the –4.9 s graph shows the irradiated region on the cell cortex. The white and black arrowheads show two minor peaks along both cell sides near the irradiation site. Two additional cells analyzed in a similar way are shown in Supplementary Figure S4.

rear of the cell was evident in the first image, which was scanned between 0.9 and 5.5 s after the irradiation. More specifically, the red fluorescence image of the rear end of this cell was scanned at 3.9 s after the start of the irradiation. The irradiated site was ~12 μm away from the rear end of the cell, implying that the red fluorescent ABD_{FLN}-mKikGR moved at a velocity faster than 3.1 μm/s. This velocity is ~9 times faster than the retrograde flow of cortical actin filaments in polarized *Dictyostelium* cells reported previously (0.34±0.15 μm/s) [6]. Ruchira *et al.* (2004) demonstrated that a diffusion coefficient (D) of GFP in a polarized *Dictyostelium* cell was 32±6 $\mu m^2/s$ [48]. Diffusion time (T_{dif}), calculated by an equation ($T_{dif} \approx x^2/2D$) was 2.3 s for 12 μm of diffusion distance x. This value is slightly shorter the interval between the irradiation and the acquisition of the first image (3.9 s), suggesting that the red fluorescent ABD_{FLN}-mKikGR mainly moved by diffusion, and specifically interacted with and was trapped by actin filaments in the rear of the cell.

In addition, there were two minor peaks of red fluorescence along both sides of the cell near the irradiation site (white arrowhead at –13.5 μm and black arrowhead at 10.5 μm from the rear end at 0.9 s after irradiation). The cell cortex around –13.5 μm was close to the irradiated area, but was not directly irradiated. Presumably cortical actin filaments in this area trapped a small fraction of red ABD_{FLN}-mKikGR generated close by. These minor peaks in polarized cells moved back to the rear relative to the cells at 0.30±0.19 μm/s (mean±S.D., n=7). These velocities are at the same level as the migration velocity of the cells (0.18±0.11 μm/s: measured at the rear end of four cells), and equivalent to the retrograde flow estimated in a previous

study (0.34±0.15 μm/s) [6]. This coincidence suggests that the red fluorescent ABD_{FLN}-mKikGR that was bound to the lateral cortical actin filaments was transported to the rear by the retrograde flow of cortical actin filaments. Apparently, total amounts of red fluorescence of ABD_{FLN}-mKikGR increased gradually over the time course of 15 s after the irradiation (Fig 2, Supplementary Figs. S4 and S5). This is presumably because fractions of newly generated red ABD_{FLN}-mKikGR was initially in the cytoplasm or bound to the dorsal or ventral cortex outside the thin confocal plane, and these fractions gradually became detectable as it bound to the side cortices or transported to the rear end, which was in the confocal plane.

Localization of ABD_{ACTN}-mKikGR

We next followed the translocation of ABD_{ACTN} using the same method as above. Green fluorescent ABD_{ACTN}-mKikGR showed stronger localization along the cortex and in the lamellipodia, and weaker distribution in the cytoplasm, than ABD_{ACTN}-GFP (Fig. 3A and Supplementary Fig. S6). Red fluorescent ABD_{ACTN}-mKikGR was undetectably low before irradiation with 405 nm light (Fig. 3B). This is presumably because the local concentration of ABD_{ACTN}-mKikGR never reached the levels of ABD_{FLN}-mKikGR at the rear of a cell, and consequently, the red fluorescence of ABD_{ACTN}-mKikGR rarely exceeded the background. After irradiation with 405 nm light near the center of the cell, red fluorescent ABD_{ACTN}-mKikGR spread along the length of the cell, with slight enrichment along the cortex (Fig. 3, B and C). The red fluorescence was somewhat stronger in the central region at 1.2 s after irradiation, but was nearly uniform along the cell length at 10.4 s. The localization of green and red fluorescence of ABD_{ACTN}-mKikGRs were eventually similar at ~33.4 s after irradiation (Fig. 3D). This localization is in sharp contrast to that of ABD_{FLN}-mKikGR, which was rapidly and specifically translocated to the rear of the cell.

Localization of actin filaments

In polarized cells expressing ABD_{FLN}-GFP, actin filaments were abundant in the lamellipodia, localized along the entire cortex, and enriched in the front and rear (Fig. 1E). However, because ABD_{FLN}-mKikGR showed much stronger posterior accumulation (Fig. 2A) than ABD_{FLN}-GFP (Fig. 1A: top), it was possible that the expression of ABD_{FLN}-mKikGR drove the accumulation of actin filaments at the rear, and ABD_{FLN}-mKikGR simply co-localized with these actin filaments. To rule out this possibility, localization of actin filaments was observed in cells expressing ABDs-mKikGR using two methods. First, mCherry-lifeact was co-expressed with ABD_{FLN}-mKikGR, and was observed simultaneously with the green fluorescence of ABD_{FLN}-mKikGR. As shown in Figure 4A, ABD_{FLN}-mKikGR was exclusively localized in the rear of the cell, while actin filaments were localized not only in the rear, but also in lamellipodia at the front. Second, polarized cells expressing ABD_{FLN}-mKikGR were fixed with glutaraldehyde and formaldehyde, and their actin filaments were stained with rhodamine-phalloidin (Fig. 4B). The staining patterns were largely consistent with live-cell imaging of ABD_{FLN}-mKikGR and mCherry-lifeact, except that cytoplasmic staining with rhodamine-phalloidin was very weak.

Localization of actin filaments in cells expressing ABD_{ACTN}-mKikGR was also observed using the same two methods (Fig. 4, C and D). The localization of actin filaments was similar to that in cells expressing ABD_{FLN}-mKikGR or in cells expressing ABD_{FLN}-GFP or ABD_{ACTN}-GFP. These results suggest that the expression of ABD-mKikGR does not noticeably influence the localization of actin filaments, and it was clear that ABD_{FLN} preferentially localizes at the rear of polarized cells even though actin filaments are abundant, not only in the rear of cells, but also in lamellipodia at the front of cells.

GAPA hardly influences the localization of ABD_{FLN}

Although ABD_{FLN} is a relatively small domain (240 amino acids) with a high affinity for actin filaments, some other protein that is localized at the rear of polarized cells may also bind to ABD_{FLN} and mediate its posterior localization. GAPA, an IQGAP-related protein of *D. discoideum*, is the only other protein that has been shown or suggested to bind to ABD_{FLN} [49]. We thus observed the localization of GFP-GAPA in polarized wild type cells, and that of ABD_{FLN} in polarized GAPA-null cells (Fig. 5 and Supplementary Fig. S7). GFP-GAPA localized at the lamellipodia and weakly along the cortex in polarized cells, and posterior enrichment of GFP-GAPA was rarely observed (Fig. 5, A and B). Moreover, ABD_{FLN}-mKikGR localized at the rear of polarized GAPA-null cells. When ABD_{FLN}-mKikGR in the middle of a polarized GAPA-null cell was photoswitched by irradiation with the 405 nm laser, red fluorescent ABD_{FLN}-mKikGR was rapidly and specifically localized at the rear of the cell (Fig. 5, C–F), as occurred in wild type cells (Fig. 2). These results demonstrate that GAPA hardly influences the localization of ABD_{FLN} in polarized cells.

Discussion

In this study, we revealed two separate mechanisms with distinct velocities for the translocation of ABD_{FLN} from the cytosol to the rear of a polarized cell. Even though actin filaments were abundant in the front of a cell, the majority of red fluorescent ABD_{FLN}-mKikGR newly generated in the middle of an elongated cell moved very rapidly to the rear, but not to the front. The speed of this translocation was ~9 times faster than the retrograde flow of cortical actin filaments. In contrast, the speed of the translocation was similar to that of diffusion of GFP, and therefore, we concluded that this translocation depends on diffusion, rather than on active transport. ABD_{ACTN}, which is homologous to ABD_{FLN}, showed the same distribution as actin filaments, strongly supporting

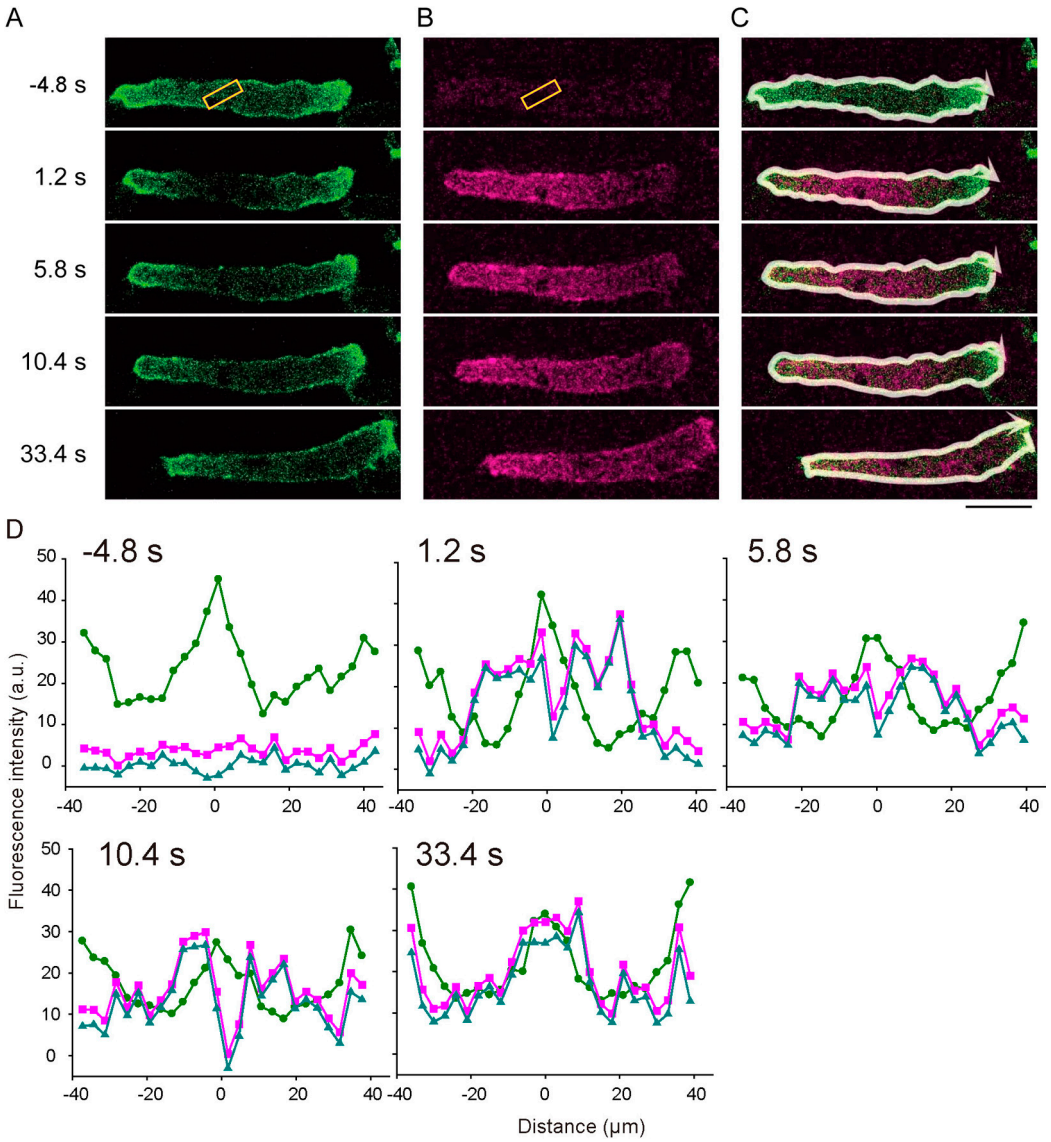

Figure 3 Translocation of ABD_{ACTN}-mKikGR. Time lapse images of a polarized cell expressing ABD_{ACTN}-mKikGR and migrating toward the right (A, B and C). (A) and (B) show the green and red fluorescence image of mKikGR, respectively, and (C) shows the merged images. The region bound by the yellow square was irradiated by 405 nm laser light for 0.7 s immediately after taking the pre-irradiation image (–4.8 s). Scanning for the subsequent images were started at 1.2, 5.8, 10.4, and 33.4 s after starting the 405 nm laser irradiation set as 0 s. Scale bar: 10 μm. (D) Profile of fluorescence intensity along the cortex, measured along the white arrows in the merged image (width: 1 μm) in (C), with 0 μm set at the rear end. The green and magenta lines show green and red fluorescence intensity of ABD_{ACTN}-mKikGR, respectively. The cyan lines show red fluorescence intensities of ABD_{ACTN}-mKikGR after subtracting the fluorescence intensities in the red channel that were unrelated to stimulated photoswitching. Two additional cells analyzed in a similar way are shown in Supplementary Figure S6.

the argument against the possibility that some other ABD that competes with ABD_{FLN} for actin binding inhibits ABD_{FLN} from localizing at the front of the cell. It is also evident that the physical size of ABD_{FLN}-GFP or ABD_{FLN}-mKikGR should not hinder its penetration into the actin meshwork at the front of the cell. Taken together, it is suggested that ABD_{FLN} diffusing in the cytoplasm recognized some feature(s) of actin filaments in the rear of the cell and interacted specifically with these filaments (diffusion and specific capture mechanism, Fig. 6A). It is beyond the scope of this study to elucidate the molecular mechanism of the specific binding between ABD_{FLN} and the posterior actin filaments. However, we and others have proposed that certain ABDs can distinguish actin filaments with different conformations. This hypothesis is based on recent discoveries that actin filaments are inherently polymorphic [32,50], and that external stimuli, including interactions with certain ABPs and mechanical tension, further expands the repertoire of conformational variations [22,23,26,27,30,51–54]. Naturally, actin filaments with different conformations would have different affinities for each ABD. Indeed, stretched actin filaments have a lower affinity for cofilin *in vivo* and *in vitro*, and a

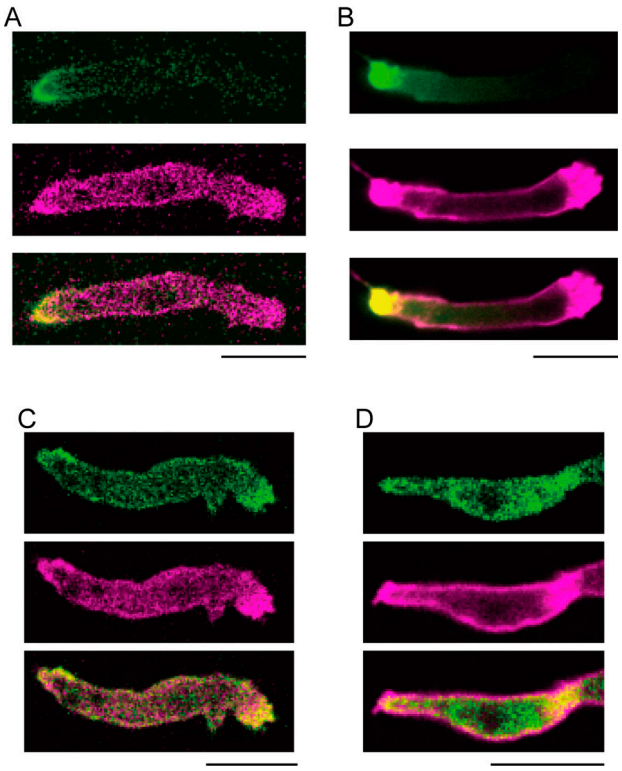

Figure 4 Localization of actin filaments in cells expressing ABD-mKikGR. (A and C) Fluorescence micrographs of polarized cells expressing ABD_{FLN}-mKikGR and mCherry-lifeact (A), or ABD_{ACTN}-mKikGR and mCherry-lifeact (C). The top and middle of each set show fluorescence images of mKikGR and mCherry, respectively, and the bottom of each set is the merged image of the two. (B and D) Permeabilized and fixed polarized cells expressing ABD_{FLN}-mKikGR (B) or ABD_{ACTN}-mKikGR (D) stained with rhodamine-phalloidin. The top and middle images show fluorescence of mKikGR and rhodamine, respectively, and the bottom of each set is the merged image of the two. All cells migrated toward the right. Scale bars: 10 μm.

higher affinity for the motor domain of myosin II *in vivo* [5,28,34]. Furthermore, certain ABPs also localize in regions where the structure of actin filaments is changed *in vivo*. For example, when a cell is aspirated locally by a microcapillary, myosin II and filamin accumulate at the aspirated site where actin filaments are tensed and bent [5,13,33,34,55]. In a polarized cell, myosin II and filamin mainly colocalize with posterior actin filaments. Those posterior actin filaments should be stretched by a pulling force exerted by myosin II filaments, unlike those in the front that should be compressed and bent by a pushing force for migration. We thus propose that ABD_{FLN} can recognize the stretched conformation of actin filaments, and specifically binds to them. Irrespective of these proposals, our findings strongly suggest that filamin can distinguish some feature of actin filaments in the rear of a cell, and this contributes to the specific localization of filamin in cells.

In the second mechanism, which is relatively minor based on the red fluorescence intensity of ABD_{FLN}-mKikGR, ABD_{FLN} that strongly interacts with actin filaments in the lateral cortex is carried to the rear of the cell by a retrograde flow of the cortical actin filaments (Fig. 6B). Ratios of fluorescence intensities between the cytosol and cortex (Supplementary Fig. S3) suggest that association of ABD_{FLN} with cortical actin filaments is stronger than that of ABD_{ACTN}, and this may be one reason why ABD_{ACTN} does not accumulate in the rear, as weakly interacting ABD_{ACTN} cannot be stably carried to the rear by this cortical flow. It should be noted, however, that ABD_{FLN} is not stably carried to the rear by binding to one actin filament, because the turnover of cortical actin filaments is very rapid during retrograde flow. For instance, based on a FRAP experiment using GFP-ABD_{FLN} as the fluorescent probe, Yumura *et al*. (2013) reported that the recovery half-time was only 0.62±0.12 s [6]. This is much shorter than the time required to carry ABD_{FLN}-mKikGR from the middle to the rear of a polarized cell at a rate of 0.34±0.15 μm/s. Furthermore, in the presence of jasplakinolide, a membrane-permeable actin-stabilizer, the half-time of fluorescence recovery was 1.82±0.39 s, which represents the off-rate of GFP-ABD_{FLN} from cortical actin filaments. This is three times slower than the recovery rate in the absence of jasplakinolide, implying that cortical actin filaments turn over before bound GFP-ABD_{FLN} dissociates [6]. Lemieux *et al*. (2014) have shown that artificially dimeric ABD_{FLN} localizes to the rear of a cell, although monomeric ABD_{FLN} does not appreciably localize there [20]. GFP tends to form a dimer weakly and it is believed that certain linker sequences between GFP and the fusion partner enhance dimerization [20,56,57]. mKikGR is reportedly a monomeric fluorescent protein while the parent KikGR forms tetramers [40]. Therefore, if mKikGR retains a weak tendency to form oligomers, ABD_{FLN}-mKikGR in this study (Fig. 2) might be assembled to oligomers by the influence of the fused proteins and/or the linker peptide. Since the oligomerized ABD_{FLN} can remain tethered to the cortical actin meshwork more stably than the monomeric ABD_{FLN} even when actin filaments turnover rapidly, oligomeric ABD_{FLN} may be transported to the rear of a cell by the retrograde flow of cortical actin filaments more efficiently than monomeric ABD_{FLN}. The ABD_{FLN}-GFP in this study (Fig. 1) might not be significantly assembled to an oligomer and is thus primarily translocated to the rear of the cells by diffusion and a specific capture mechanism. This is because our linker peptide is not hydrophobic and the posterior localization of ABD_{FLN}-GFP was weaker than that of ABD_{FLN}-mKikGR. This cortical actin flow mechanism is presumably physiologically relevant, however, since the parent molecules, filamin and α-actinin, are naturally dimers.

It is possible that these two mechanisms contribute to the localization of various other ABPs *in vivo*. In particular, if actin filaments at different sites in a cell have unique structural features caused by biochemical modulation, nucleotide state, ABP binding, tension, twisting or bending, the diffusion and specific capture mechanism can be applied to ABP localization at various sites in a cell. Since differential local-

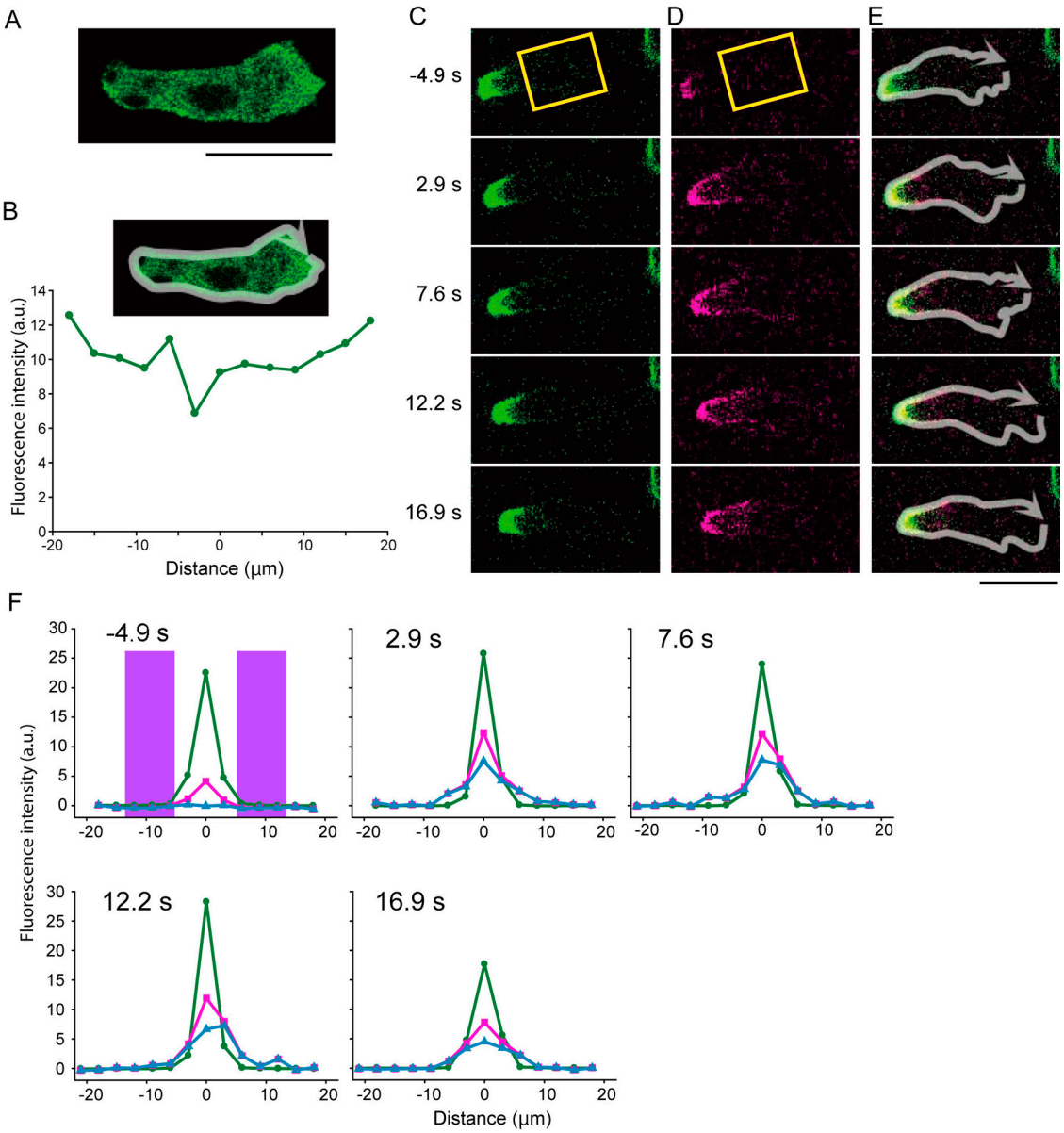

Figure 5 Localization of GAPA and translocation of ABD_{FLN}-mKikGR in a GAPA null cell. (A) Fluorescence micrographs of a polarized cell expressing GFP-GAPA. The cell migrated toward the right of the images. (B) Intensity profile of GFP along the cortex, measured along the white line in the direction of the arrow in the inserted image (same as A). Another representative cell is shown in Supplementary Figure S7, A and B. (C–E) Time lapse images of a GAPA null cell expressing ABD_{FLN}-mKikGR and migrating toward the right. (C) and (D) show the green and red fluorescence images of mKikGR, respectively, and (E) shows the merged images. The region bound by the yellow square was irradiated by 405 nm laser light for 2.4 s immediately after taking the pre-irradiation image (–4.9 s). Scanning of the subsequent images were started at 2.9, 7.6, 12.2, and 16.9 s after starting the 405 nm irradiation set as 0 s. Scale bars: 10 μm. (F) Profiles of fluorescence intensities along the cell cortex in the region and direction shown by the white arrows in (E), with the 0 μm set at the rear end. The green and magenta lines show fluorescence intensities of ABD_{FLN}-mKikGR in the green and red channels, respectively. The cyan line shows red fluorescence intensity of ABD_{FLN}-mKikGR after subtracting the fluorescence intensity in the red channel that was unrelated to the stimulated photoswitch. The purple vertical bars in the –4.9 s graph shows the irradiated region on the cell cortex. Two additional cells analyzed in a similar way are shown in Supplementary Figure S7 C–J.

ization of multiple ABPs to specific actin filaments in cells leads to functional differentiation of actin filaments, it is important to elucidate the mechanisms by which ABPs recognize structural features of actin filaments.

Acknowledgments

This work was supported in part by a Grant-in-Aid from the Ministry of Education, Culture, Sports, Science and Technology No. 24117008 to TU.

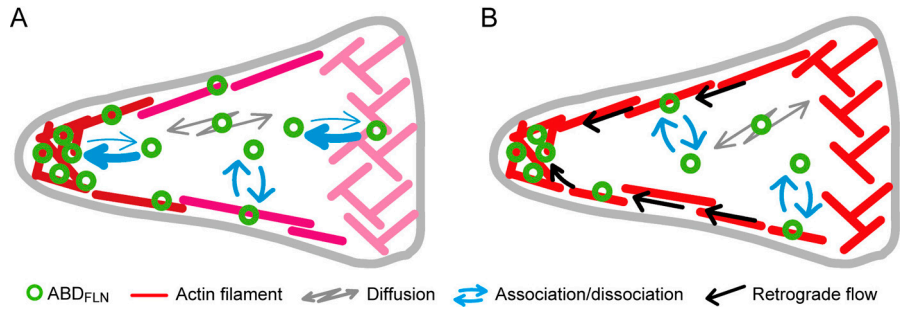

Figure 6 Schematic illustration of the two mechanisms of ABD_{FLN} translocation from the cytosol in the middle to the rear cortex of a polarized cell. (A) Diffusion and specific capture mechanism. The affinity between actin filaments and ABD_{FLN} differs depending on the position in the cell, as indicated by the graded intensity of the red color of actin filaments. Since the affinity of the rear actin filaments for ABD_{FLN} is stronger than other actin filaments, ABD_{FLN} that is rapidly diffusing in the cytoplasm is specifically captured by the rear actin filaments and accumulates there. (B) Cortical actin flow mechanism. Cytosolic ABD_{FLN} interacts with cortical actin filaments and is carried to the rear of the cell by retrograde flow (black arrows) of the cortical actin filaments. In both schemes, the front of the cell is to the right.

Conflicts of Interest

All the authors declare that they have no conflict of interest.

Author Contributions

K. S. and T. U. conceived and planned the experiments. K. S., A. N. and T. U. performed the experiments. K. S. analyzed the data. K. S., A. N., H. A. and T. U. contributed reagents and materials. K. S., H. A. and T. U. wrote the manuscript. All the authors reviewed the result and agreed the final manuscript.

References

[1] Pantaloni, D., Le Clainche, C. & Carlier, M. F. Mechanism of actin-based motility. *Science* **292**, 1502–1506 (2001).
[2] Small, J. V., Stradal, T., Vignal, E. & Rottner, K. The lamellipodium: where motility begins. *Trends Cell Biol.* **12**, 112–120 (2002).
[3] Le Clainche, C. & Carlier, M. F. Regulation of actin assembly associated with protrusion and adhesion in cell migration. *Physiol. Rev.* **88**, 489–513 (2008).
[4] Pollard, T. D. & Cooper, J. A. Actin, a central player in cell shape and movement. *Science* **326**, 1208–1212 (2009).
[5] Uyeda, T. Q. P., Iwadate, Y., Umeki, N., Nagasaki, A. & Yumura, S. Stretching actin filaments within cells enhances their affinity for the myosin II motor domain. *PLoS ONE* **6**, e26200 (2011).
[6] Yumura, S., Itoh, G., Kikuta, Y., Kikuchi, T., Kitanishi-Yumura, T. & Tsujioka, M. Cell-scale dynamic recycling and cortical flow of the actin-myosin cytoskeleton for rapid cell migration. *Biol. Open* **2**, 200–209 (2013).
[7] DeBiasio, R. L., LaRocca, G. M., Post, P. L. & Taylor, D. L. Myosin II transport, organization, and phosphorylation: evidence for cortical flow/solation-contraction coupling during cytokinesis and cell locomotion. *Mol. Biol. Cell* **7**, 1259–1282 (1996).
[8] Henson, J. H., Svitkina, T. M., Burns, A. R., Hughes, H. E., MacPartland, K. J., Nazarian, R., *et al.* Two components of actin-based retrograde flow in sea urchin coelomocytes. *Mol. Biol. Cell* **10**, 4075–4090 (1999).
[9] Yumura, S. Myosin II dynamics and cortical flow during contractile ring formation in Dictyostelium cells. *J. Cell Biol.* **154**, 137–146 (2001).
[10] Renkawitz, J., Schumann, K., Weber, M., Lämmermann, T., Pflicke, H., Piel, M., *et al.* Adaptive force transmission in amoeboid cell migration. *Nat. Cell Biol.* **11**, 1438–1443 (2009).
[11] Byfield, F. J., Wen, Q., Levental, I., Nordstrom, K., Arratia, P. E., Miller, R. T., *et al.* Absence of filamin A prevents cells from responding to stiffness gradients on gels coated with collagen but not fibronectin. *Biophys. J.* **96**, 5095–5102 (2009).
[12] Lynch, C. D., Gauthier, N. C., Biais, N., Lazar, A. M., Roca-Cusachs, P., Yu, C. H., *et al.* Filamin depletion blocks endoplasmic spreading and destabilizes force-bearing adhesions. *Mol. Biol. Cell* **22**, 1263–1273 (2011).
[13] Luo, T., Mohan, K., Iglesias, P. A. & Robinson, D. N. Molecular mechanisms of cellular mechanosensing. *Nat. Mater.* **12**, 1064–1071 (2013).
[14] Sun, C., Forster, C., Nakamura, F. & Glogauer, M. Filamin-A Regulates Neutrophil Uropod Retraction through RhoA during Chemotaxis. *PLoS ONE* **8**, e79009 (2013).
[15] McCoy, A. J., Fucini, P., Noegel, A. A. & Stewart, M. Structural basis for dimerization of the Dictyostelium gelation factor (ABP120) rod. *Nat. Struct. Biol.* **6**, 836–841 (1999).
[16] Nakamura, F., Stossel, T. P. & Hartwig, J. H. The filamins: organizers of cell structure and function. *Cell Adh. Migr.* **5**, 160–169 (2011).
[17] Bretschneider, T., Diez, S., Anderson, K., Heuser, J., Clarke, M., Müller-Taubenberger, A., *et al.* Dynamic actin patterns and Arp2/3 assembly at the substrate-attached surface of motile cells. *Curr. Biol.* **14**, 1–10 (2004).
[18] Lénárt, P., Bacher, C. P., Daigle, N., Hand, A. R., Eils, R., Terasaki, M., *et al.* A contractile nuclear actin network drives chromosome congression in oocytes. *Nature* **436**, 812–818 (2005).
[19] Washington, R. W. & Knecht, D. A. Actin binding domains direct actin-binding proteins to different cytoskeletal locations. *BMC Cell Biol.* **9**, 10 (2008).
[20] Lemieux, M. G., Janzen, D., Hwang, R., Roldan, J., Jarchum, I. & Knecht, D. A. Visualization of the actin cytoskeleton: different F-actin-binding probes tell different stories. *Cytoskeleton (Hoboken).* **71**, 157–169 (2014).
[21] Ciobanasu, C., Faivre, B. & Le Clainche, C. Integrating actin dynamics, mechanotransduction and integrin activation: the multiple functions of actin binding proteins in focal adhesions. *Eur. J. Cell Biol.* **92**, 339–348 (2013).

[22] Loscalzo, J., Reed, G. H. & Weber, A. Conformational change and cooperativity in actin filaments free of tropomyosin. *Proc. Natl. Acad. Sci. USA* **72**, 3412–3415 (1975).
[23] Matsushita, S., Inoue, Y., Hojo, M., Sokabe, M. & Adachi, T. Effect of tensile force on the mechanical behavior of actin filaments. *J. Biomech.* **44**, 1776–1781 (2011).
[24] Hanein, D., Matsudaira, P. & DeRosier, D. J. Evidence for a conformational change in actin induced by fimbrin (N375) binding. *J. Cell Biol.* **139**, 387–396 (1997).
[25] Huang, R., Grabarek, Z. & Wang, C. L. A. Differential effects of caldesmon on the intermediate conformational states of polymerizing actin. *J. Biol. Chem.* **285**, 71–79 (2010).
[26] McGough, A., Pope, B., Chiu, W. & Weeds, A. Cofilin changes the twist of F-actin: implications for actin filament dynamics and cellular function. *J. Cell Biol.* **138**, 771–781 (1997).
[27] Tsaturyan, A. K., Koubassova, N., Ferenczi, M. A., Narayanan, T., Roessle, M. & Bershitsky, S. Y. Strong binding of myosin heads stretches and twists the actin helix. *Biophys. J.* **88**, 1902–1910 (2005).
[28] Hayakawa, K., Tatsumi, H. & Sokabe, M. Actin filaments function as a tension sensor by tension-dependent binding of cofilin to the filament. *J. Cell Biol.* **195**, 721–727 (2011).
[29] Sharma, S., Grintsevich, E. E., Phillips, M. L., Reisler, E. & Gimzewski, J. K. Atomic force microscopy reveals drebrin induced remodeling of f-actin with subnanometer resolution. *Nano Lett.* **11**, 825–827 (2011).
[30] Ngo, K. X., Kodera, N., Katayama, E., Ando, T. & Uyeda, T. Q. P. Cofilin-induced unidirectional cooperative conformational changes in actin filaments revealed by high-speed atomic force microscopy. *Elife* **4**, e04806 (2015).
[31] Sharma, S., Grintsevich, E. E., Hsueh, C., Reisler, E. & Gimzewski, J. K. Molecular cooperativity of drebrin1-300 binding and structural remodeling of F-actin. *Biophys. J.* **103**, 275–283 (2012).
[32] Galkin, V. E., Orlova, A., Schröder, G. F. & Egelman, E. H. Structural polymorphism in F-actin. *Nat. Struct. Mol. Biol.* **17**, 1318–1323 (2010).
[33] Merkel, R., Simson, R., Simson, D. A., Hohenadl, M., Boulbitch, A., Wallraff, E., *et al.* A micromechanic study of cell polarity and plasma membrane cell body coupling in Dictyostelium. *Biophys. J.* **79**, 707–719 (2000).
[34] Kim, J. H., Ren, Y., Ng, W. P., Li, S., Son, S., Kee, Y. S., *et al.* Mechanical tension drives cell membrane fusion. *Dev. Cell* **32**, 561–573 (2015).
[35] Ren, Y., Effler, J. C., Norstrom, M., Luo, T., Firtel, R. A., Iglesias, P. A., *et al.* Mechanosensing through cooperative interactions between myosin II and the actin crosslinker cortexillin I. *Curr. Biol.* **19**, 1421–1428 (2009).
[36] Stock, A., Steinmetz, M. O., Janmey, P. A., Aebi, U., Gerisch, G., Kammerer, R. A., *et al.* Domain analysis of cortexillin I: actin-bundling, PIP(2)-binding and the rescue of cytokinesis. *EMBO J.* **18**, 5274–5284 (1999).
[37] Vignjevic, D., Kojima, S., Aratyn, Y., Danciu, O., Svitkina, T. & Borisy, G. G. Role of fascin in filopodial protrusion. *J. Cell Biol.* **174**, 863–875 (2006).
[38] Takahashi, H., Sekino, Y., Tanaka, S., Mizui, T., Kishi, S. & Shirao, T. Drebrin-dependent actin clustering in dendritic filopodia governs synaptic targeting of postsynaptic density-95 and dendritic spine morphogenesis. *J. Neurosci.* **23**, 6586–6595 (2003).
[39] Ngo, K. X., Umeki, N., Kijima, S. T., Kodera, N., Ueno, H., Furutani-Umezu, N., *et al.* Allosteric regulation by cooperative conformational changes of actin filaments drives mutually exclusive binding with cofilin and myosin. *Sci. Rep.* **6**, 1–11 (2016).
[40] Habuchi, S., Tsutsui, H., Kochaniak, A. B., Miyawaki, A. & van Oijen, A. M. mKikGR, a monomeric photoswitchable fluorescent protein. *PLoS ONE* **3**, e3944 (2008).
[41] Levi, S., Polyakov, M. & Egelhoff, T. T. Green fluorescent protein and epitope tag fusion vectors for Dictyostelium discoideum. *Plasmid* **44**, 231–238 (2000).
[42] Riedl, J., Crevenna, A. H., Kessenbrock, K., Yu, J. H., Neukirchen, D., Bista, M., *et al.* Lifeact: a versatile marker to visualize F-actin. *Nat. Methods* **5**, 605–607 (2008).
[43] Asano, Y., Mizuno, T., Kon, T., Nagasaki, A., Sutoh, K. & Uyeda, T. Q. P. Keratocyte-like locomotion in amiB-null Dictyostelium cells. *Cell Motil. Cytoskeleton* **59**, 17–27 (2004).
[44] Adachi, H., Takahashi, Y., Hasebe, T., Shirouzu, M., Yokoyama, S. & Sutoh, K. Dictyostelium IQGAP-related protein specifically involved in the completion of cytokinesis. *J. Cell Biol.* **137**, 891–898 (1997).
[45] Sussman, M. Cultivation and synchronous morphogenesis of Dictyostelium under controlled experimental conditions. *Methods Cell Biol.* **28**, 9–29 (1987).
[46] Egelhoff, T. T., Titus, M. A., Manstein, D. J., Ruppel, K. M. & Spudich, J. A. Molecular genetic tools for study of the cytoskeleton in Dictyostelium. *Methods Enzymol.* **196**, 319–334 (1991).
[47] Yumura, S., Mori, H. & Fukui, Y. Localization of actin and myosin for the study of ameboid movement in Dictyostelium using improved immunofluorescence. *J. Cell Biol.* **99**, 894–899 (1984).
[48] Ruchira, Hink, M. A., Bosgraaf, L., van Haastert, P. J. M. & Visser, A. J. W. G. Pleckstrin homology domain diffusion in Dictyostelium cytoplasm studied using fluorescence correlation spectroscopy. *J. Biol. Chem.* **279**, 10013–10019 (2004).
[49] Mondal, S., Burgute, B., Rieger, D., Müller, R., Rivero, F., Faix, J., *et al.* Regulation of the actin cytoskeleton by an interaction of IQGAP related protein GAPA with filamin and cortexillin I. *PLoS ONE* **5**, e15440 (2010).
[50] Egelman, E. H., Francis, N. & DeRosier, D. J. F-actin is a helix with a random variable twist. *Nature* **298**, 131–135 (1982).
[51] Galkin, V. E., Orlova, A. & Egelman, E. H. Actin filaments as tension sensors. *Curr. Biol.* **22**, R96-101 (2012).
[52] Miki, M., Wahl, P. & Auchet, J. C. Fluorescence anisotropy of labeled F-actin: influence of divalent cations on the interaction between F-actin and myosin heads. *Biochemistry* **21**, 3661–3665 (1982).
[53] Ressad, F., Didry, D., Xia, G. X., Hong, Y., Chua, N. H., Pantaloni, D., *et al.* Kinetic analysis of the interaction of actin-depolymerizing factor (ADF)/cofilin with G- and F-actins. Comparison of plant and human ADFs and effect of phosphorylation. *J. Biol. Chem.* **273**, 20894–20902 (1998).
[54] Galkin, V. E., Orlova, A., Lukoyanova, N., Wriggers, W. & Egelman, E. H. Actin depolymerizing factor stabilizes an existing state of F-actin and can change the tilt of F-actin subunits. *J. Cell Biol.* **153**, 75–86 (2001).
[55] Pramanik, M. K., Iijima, M., Iwadate, Y. & Yumura, S. PTEN is a mechanosensing signal transducer for myosin II localization in Dictyostelium cells. *Genes Cells* **14**, 821–834 (2009).
[56] Yang, F., Moss, L. G. & Phillips, G. N. The molecular structure of green fluorescent protein. *Nat. Biotechnol.* **14**, 1246–1251 (1996).
[57] Zacharias, D. A., Violin, J. D., Newton, A. C. & Tsien, R. Y. Partitioning of lipid-modified monomeric GFPs into membrane microdomains of live cells. *Science* **296**, 913–916 (2002).